Author Manuscript

Author Manuscript

Author Manuscript

Author Manuscript

HHS Public Access

Author manuscript

Exp Eye Res. Author manuscript; available in PMC 2017 August 01.

Published in final edited form as:

Exp Eye Res. 2016 August ; 149: 16–25. doi:10.1016/j.exer.2016.05.028.

Development of diabetes-induced acidosis in the rat retina

Andrey V. Dmitriev[1], **Desmond Henderson**[1], and **Robert A. Linsenmeier**[1,2,3]

Andrey V. Dmitriev: andrey.dmitriev@northwestern.edu; Desmond Henderson: d-henderson@northwestern.edu

[1]Department of Biomedical Engineering, 2145 Sheridan Road, Northwestern University, Evanston, IL, 60208-3107, United States

[2]Department of Neurobiology, 2205 Tech Drive, Northwestern University, Evanston, IL, 60208, United States

[3]Department of Ophthalmology, Northwestern University, 645 North Michigan Avenue, Suite 440, Chicago, IL 60611, United States

Abstract

We hypothesized that the retina of diabetic animals would be unusually acidic due to increased glycolytic metabolism. Acidosis in tumors and isolated retina has been shown to lead to increased VEGF. To test the hypothesis we have measured the transretinal distribution of extracellular H^+ concentration (H^+-profiles) in retinae of control and diabetic dark-adapted intact Long-Evans rats with ion-selective electrodes. Diabetes was induced by intraperitoneal injection of streptozotocin. Intact rat retinae are normally more acidic than blood with peak of $[H^+]_o$ in the outer nuclear layer (ONL) that averages 30 nM higher than H^+ in the choroid. Profiles in diabetic animals were similar in shape, but diabetic retinae began to be considerably more acidic after 5 weeks of diabetes. In retinae of 1 to 3 month diabetics the difference between the ONL and choroid was almost twice as great as in controls. At later times, up to 6 months, some diabetics still demonstrated abnormally high levels of $[H^+]_o$, but others were even less acidic than controls, so that the average level of acidosis was not different. Greater variability in H^+-profiles (both between animals and between profiles recorded in one animal) distinguished the diabetic retinae from controls. Within animals, this variability was not random, but exhibited regions of higher and lower H^+. We conclude that retinal acidosis begins to develop at an early stage of diabetes (1 to 3 months) in rats. However, it does not progress, and the acidity of diabetic rat retina was diminished at later stages (3 to 6 months). Also the diabetes-induced acidosis has a strongly expressed local character. As result, the diabetic retinas show much wider variability in $[H^+]$ distribution than controls. pH influences metabolic and neural processes, and these results suggest that local acidosis could play a role in the pathogenesis of diabetic retinopathy.

Corresponding author: Robert A. Linsenmeier, r-linsenmeier@northwestern.edu.

Publisher's Disclaimer: This is a PDF file of an unedited manuscript that has been accepted for publication. As a service to our customers we are providing this early version of the manuscript. The manuscript will undergo copyediting, typesetting, and review of the resulting proof before it is published in its final citable form. Please note that during the production process errors may be discovered which could affect the content, and all legal disclaimers that apply to the journal pertain.

Disclosure

The authors have no financial interests to disclose.

Author Manuscript Author Manuscript Author Manuscript Author Manuscript

Keywords

pH; acidosis; diabetes; streptozotocin; rat; ion-selective microelectrodes; retina

1. Introduction

While there has been a great deal of work and speculation about changes in oxygen in the diabetic retina, very little is known about another important metabolic parameter, pH. The possibility that acidosis contributes to some of the pathogenesis of diabetic retinopathy is supported by several lines of evidence. First, VEGF, which is acknowledged to be an important player in diabetic retinopathy (Stitt et al., 2015), is known to be upregulated by acidosis independently of hypoxia in glioblastoma (Xu et al., 2002) and pancreatic adenocarcinoma (Fukumura et al., 2001; Shi et al., 2001). VEGF also increases when the isolated rat retina is subjected to acidosis (Zhu et al., 2009). Second, in neonatal retina acidosis can mimic the effect of oxygen-induced retinopathy in causing neovascularization (Holmes et al., 1998, 1999; Leske et al., 2004). Third, acute hyperglycemia markedly acidified the normal cat retina (Padnick-Silver and Linsenmeier, 2005), particularly the inner retina. Thus, we can hypothesize that the hyperglycemia in diabetes increases anaerobic glycolysis and the consequent production of lactate and H^+, and that this could contribute to an increase VEGF, causing at least part of the neovascularization in diabetes, not to mention the many other changes that could occur in retinal function due to acidosis. The only measurements of intraretinal pH in diabetic animals, however, were those made on a very small number of diabetic cats, most of which had long-standing diabetes (7.7 to 9.4 years) with considerable capillary dropout (Budzynski et al., 2005). The findings in those animals were puzzling. In a normal animal, the point of highest $[H^+]_o$ in the retina is in the outer nuclear layer, with decreasing H^+ toward the choroid and toward the vitreous. In many profiles in the long-term diabetics, the inner retina was the most acidic part of the retina, and the outer retina did not exhibit the usual high value of H^+. We hypothesized that failure of photoreceptor glycolysis had also occurred, which reduced H^+ production, as the photoreceptors are affected in diabetes (Kern and Berkowitz, 2015; Scarinci et al., 2015). In one cat with only 2.1 years of diabetes the shape of the H^+ profiles was more normal, and the major change was acidification (Budzynski et al., 2005), as we had originally expected. However, the fact remains that there have been very limited measurements. It has not been possible previously to study how retinal pH changes over time in diabetic animals, and how $[H^+]_o$ gradients are altered as the disease progresses. The only other work to date on retinal H^+ in diabetes has been our recent study on changes in intraretinal $[H^+]_o$ evoked by flashes of light (Dmitriev et al., 2016). Light-evoked responses were altered only distal to the RPE in the choroid, suggesting possible dysfunction in the ability of the choroid to clear H^+ from the retina during diabetes.

The present study was therefore undertaken to close the gap in basic knowledge about retinal pH in diabetes. Because it is difficult to study diabetes in a large animal model, we measured intraretinal profiles of $[H^+]_o$ in vivo with H^+-sensitive microelectrodes in diabetic rats at different time points up to 27 weeks after the induction of diabetes, and compared the findings to those in age-matched control animals. Our hypothesis was that the diabetics

Author Manuscript Author Manuscript Author Manuscript Author Manuscript

would be more acidic than controls during at least some period of time, although possibly not continuously, based on what had been observed in cat (Budzynski et al., 2005). Further, because of the work on acute hyperglycemia in cats, we expected especially the inner retina to be more acidic than normal. These hypotheses were partly supported by the data.

2. Material and Methods

2.1 Animal preparation

Animal experiments were performed in accordance with the Association for Research in Vision and Ophthalmology Statement for the Use of Animals in Ophthalmic and Vision Research and were approved by Northwestern University's Institutional Animal Care and Use Committee. Adult male Long-Evans rats were anesthetized with 2.5–3% isoflurane/35% O_2 during preparation, and anesthesia was gradually switched to urethane (800 mg/kg loading followed by 75 mg-kg^{-1}-hr^{-1}) supplemented with 0.5% isoflurane. After completing surgical preparations, the animal was paralyzed with pancuronium bromide and artificially ventilated. An arterial cannula was used to measure blood pressure and to take blood samples for measurements of PaO_2, $PaCO_2$, pHa and glucose. The tidal volume provided by the respirator and the fraction of inspired oxygen were adjusted to maintain arterial values in the normal range of $P_aO_2 \approx 100$ mmHg, $P_aCO_2 \approx 40$ mmHg and pHa ≈ 7.4. The animal's body temperature was measured with a rectal probe and used to control a water filled heating pad to maintain temperature at 37° C. Needle leads were used to measure heart rate from the ECG. Further details of the preparation have been given previously (Lau and Linsenmeier, 2012). Forty-one rats (18 controls and 23 diabetics) were studied. Light-evoked H^+ responses have been reported from some of these same animals (Dmitriev et al., 2016).

2.2 Induction of diabetes

Diabetes was induced with a single intraperitoneal injection of STZ and age-matched controls received a single intraperitoneal injection of 0.05 mol/L sodium citrate buffer only as reported previously (Dmitriev et al., 2016). Rats were weighed weekly, and nonfasting blood glucose levels were measured from the tail vein using a Bayer CONTOUR Meter (Bayer HealthCare LLC, Mishawaka, IN). In diabetics, average blood glucose was 519 ± 74 mg/dL (mean ± s.d.) during weekly measurements prior to the H^+ recordings. During the experiments, the blood glucose was usually lower (in 22 out of 23 cases) and the average was 407 ± 80 mg/dL, which was still much higher than in controls (137 ± 41, n = 17). Data presented here were obtained from animals after 2 to 27 weeks (0.5 to 6 months) of diabetes.

2.3 $[H^+]_o$ recordings

Double-barreled H^+-sensitive microelectrodes used to record intraretinal $[H^+]_o$ were constructed using methods described previously for Ca^{2+}-sensitive microelectrodes (Dmitriev et al., 1999), except that the electrodes were filled with Hydrogen Ionophore I - Cocktail A or Cocktail B (Fluka). One of the barrels served to record voltage and the other contained an H^+-sensitive liquid and therefore recorded the H^+ equilibrium potential across the liquid plus voltage. Both ion-selective and reference barrels were backfilled with a simplified Ringer's solution (140 mM NaCl, 5 mM KCl, 10 mM HEPES, pH=7.4). After

Author Manuscript Author Manuscript Author Manuscript Author Manuscript

filling, the tip of the microelectrode was beveled on a micropipette beveler (BV-10, Sutter Instrument Co.) so that the tip diameter was 5–8 μm. The resistance of the H^+-selective barrel was 50 – 70 GΩ; the reference barrel had a resistance of 60 – 100 MΩ. Electrodes were calibrated in solutions that were similar to the standard Ringer's and had pH values of 7.0, 7.4 and 7.8. The slope of the H^+ electrodes was close to Nernstian. Voltage from the H^+ barrel was recorded with a high input impedance amplifier (FD-223a, WPI).

The microelectrode was placed inside a metal needle inserted into the eye through the sclera and advanced through the vitreous toward the retina as described earlier (Lau and Linsenmeier, 2012). The rat's head was adjusted so that the cornea of the right eye faced upward, and the visual axis was oriented vertically. The microelectrode penetrated the sclera on the superior side of the eye near the equator at an angle of 32° or 34° and hit the retina about 1 mm inferior to the disc. To obtain a series of H^+-profiles, the electrode was adjusted in successive penetrations by rotating it about the entry point on the eye in steps of 2° so that the penetrations covered up to 30° in the nasal to caudal direction. Both the voltage and ion-selective barrels were referenced to an Ag/AgCl electrode in the neck. When in the retina, as signaled by a change in the electroretinogram, the electrode was advanced in 30 μm steps by a hydraulic micropositioner (Kopf model 2650) until penetration of the retinal pigment epithelium. From there the electrode was continuously withdrawn at1 μm/sec back to the vitreous. The choroid/retinal boundary was considered to be the point at which $[H^+]$ began to increase. During withdrawal, short dim flashes (white light, 7.5 lux for 100 msec) were delivered at 10 sec intervals to record the intraretinal ERG. The vitreoretinal interface was identified as the location where the intraretinal ERG recorded by the voltage barrel of the microelectrode during withdrawal was the same as the vitreal ERG. To obtain the pure H^+-dependent voltages, the voltages recorded by the voltage barrel of the electrode during the withdrawal were subtracted from the simultaneously recorded voltages from the H^+-selective barrel. The resulting H^+-selective voltages (Figure 1A) were recalculated into H^+-profiles in the following 3 steps. First, the voltage of the H^+-selective microelectrode (in mV) was converted to $[H^+]$ (in nM) based on a calibration of each electrode performed before the experiment. Absolute values of extracellular H^+ concentration ($[H^+]_o$) were obtained by assuming that $[H^+]$ in the choroid during each penetration was the same as arterial $[H^+]$ measured just before or after each profile. Second, the length of the profiles, which was variable partly because of natural variations in the local retina thickness, but mostly due to different penetration angles, was normalized. The retinal borders with the choroid and vitreous were defined to be 100% and 0% retinal depth, respectively. Third, data points were averaged over each 5% of retinal depth, resulting in profiles containing 20 values. These are presented as the final H^+-profiles (Figure 1B). The amplitude of a H^+-profile was defined to be the maximum $[H^+]$ in the retina minus the value of $[H^+]$ in the choroid. The digitizing frequency during some recordings was 2 Hz, which was quite enough for slow voltage changes associated with the electrode withdrawal. However, in later experiments (about 2/3 of all) we used a 100 Hz digitizing frequency to improve resolution of the ERG recordings that assisted us in determining the vitreoretinal boundary.

All experiments were performed in dark adaptation and the short flashes of dim light mentioned above did not disturb it, as was evident from the vitreal ERG, which did not change in amplitude during the long hours (up to 10 hours) of the experiment.

Author Manuscript Author Manuscript Author Manuscript Author Manuscript

3. Results

Representative samples of H^+-profiles measured in control and diabetic rats are shown in Figure 2, where each panel presents data from one rat. H^+-profiles recorded in control rats (two top rows) were usually smooth curves that peaked at 60–65% of the retinal depth, and had slightly higher $[H^+]$ at the vitreous (0% depth) than at the choroid (100% depth) as reported previously in retinae of intact rat (Dmitriev et al., 2016) and cat (Padnick-Silver and Linsenmeier, 2002; Yamamoto et al., 1992). This distribution of H^+ in the transretinal profiles is due to 1) uneven H^+ production during energy metabolism, 2) the influence of buffering, and 3) H^+ clearance by the retinal and choroidal circulations. Mathematical modeling of H^+ profiles in cat indicated that the production of H^+, or more correctly the extrusion of H^+ into the extracellular space, was largest in the outer nuclear layer. Manipulations of the energy demand (by prolonged light or hypoxia) alter H^+ production and, accordingly, the transretinal H^+ distribution (Dmitriev et al., 2016; Padnick-Silver and Linsenmeier, 2002, 2005; Yamamoto et al., 1992; Yamamoto and Steinberg, 1992). In this paper dark adaptation was chosen as a standard condition for comparison of H^+-profiles in control and diabetic rats. In the control retinae, the amplitude of H^+-profiles, which was defined as the difference between the maximum $[H^+]_o$ in the retina and $[H^+]$ in the choroid (see Methods, Fig. 1), was usually about 30 nM (corresponding to a minimum pH = 7.16) although in a few cases the amplitude was as small as 20 nM (minimum pH = 7.22, Fig. 2B) or as high as 50 nM (minimum pH = 7.05, Fig. 2D).

Diabetic retinas often (but not always) were more acidic than controls. In the most dramatic case (Fig. 2H) the maximum $[H^+]_o$ reached 200 nM (pH = 6.7) and the amplitude of $[H^+]$ changes exceeded 160 nM. Diabetic rats also demonstrated much wider variation among their H^+-profiles compared to controls. In diabetics, H^+-profiles were variable both from animal to animal and from one profile to another within the same animal. This variability is illustrated by the examples in Fig. 2 (two bottom rows). Profiles in Fig. 2K are greatly variable in peak amplitude but have similar $[H^+]_o$ in the proximal part of the retina; profiles in Fig. 2G are similar in maximum amplitude but largely different in the proximal part of the retina; profiles in Figs. 2I and 2J are divided in two distinguishable groups; large profiles in Figs. 2H and L have an unusually sharp shape.

Average amplitudes of H^+-profiles measured in individual rats (mean ± s.d.) are plotted against time after initiation of diabetes (or injection of a vehicle for control) in Fig. 3A, with the red bars in the upper part of the figure for diabetics and the green bars in the lower part of the figure for controls. For easier visual comparison, the mean values of H^+-profiles from control (green dots) and diabetic (red dots) animals are presented together in the upper part of Fig. 3B. It is apparent that in spite of significant variability, diabetic retinae were more acidic than controls between 5 and 13 weeks (i.e. 1 to 3 months) after diabetes initiation, but not before (up to 4 weeks, i.e. less than 1 month) or after (from 14 to 27 weeks, i.e. 3 to 6 months). As already noted in the examples of Fig. 2, diabetics as a whole also demonstrated much larger variability than controls between the H^+-profile amplitudes within the same animal, especially about1 month following STZ injection. We used the standard deviation of the H^+-profile amplitudes recorded in individual rats as a measure of variability, and this is presented as a function of time in the lower part of Fig. 3B.

Author Manuscript Author Manuscript Author Manuscript Author Manuscript

Because the effect shown in Fig. 3 appeared to depend on the duration of diabetes, we compared H^+-profiles from control and diabetic rats separately for 3 time periods: shorter than 1 month, 1 to 3 months, and 3 to 6 months. Descriptive statistics for these time periods are shown in Fig. 4 as box charts. For the sake of equal representation, only 3 profiles from each rat were used. In numerous cases when more than 3 profiles were recorded in a certain rat, the amplitudes of those 3 profiles which were closest to the average for that animal were chosen. As a result, the variability in each group of data was artificially restricted to some extent. The variability was still substantial, particularly for diabetics after 1 month, as is evident from Fig. 4. The mean and median are shown by the square and solid horizontal lines, respectively; the dashed lines contain the middle half of the profiles; and the ends of the box represent the 10% and 90% values. This figure demonstrates again that the retinae of 1 – 3 month diabetic rats were considerably more acidic than the retinae of age-matched controls. The average amplitude of H^+-profiles in that period of time was 51.4 ± 5.1 nM (n = 30) for diabetics and 26.4 ± 2.1 nM (n = 15) for controls (mean ± s.e.m.). To test the statistical significance of this difference we used the nonparametric Kolmogorov-Smirnov test because the distributions were clearly not normal, which was evident from difference between means and medians, especially for diabetics after 1 month. The cumulative distributions of H^+-profile amplitudes from control and diabetic rats in the 3 different time periods is shown in Fig. 5. According to the Kolmogorov-Smirnov test the difference between average diabetic and control H^+-profile amplitudes was statistically significant ($P < 0.001$) in the 1 to 3 month period. There was no statistically significant difference between diabetics and controls during the first 4 weeks (27.9 ± 1.2 nM, n = 21 and 30.7 ± 1.3 nM, n = 15, respectively), or after 3 months of diabetes (32.9 ± 4.5 nM, n = 18 and 34.2 ± 1.7 nM, n=24). It is also noticeable that although the average amplitude of H^+-profiles of diabetics after 3 months was similar to the controls, the variation of amplitudes was greater in diabetics, and they had both the smallest and the largest values.

Until this point, our attention has been focused on the amplitudes of the H^+-profiles. To compare other parameters which characterize the transretinal H^+ distribution, average H^+-profiles were calculated for 1 – 3 months and more than 3 months of diabetes (Fig. 6, upper row; mean ± s.d.). Data for short-term diabetics (< 1 month) are not shown because they were practically the same as controls (see Fig. 4 and 5). To calculate the average H^+-profiles, the values of $[H^+]_o$ recorded at the same location but in the different rats were averaged. The same 3 representative profiles per rat that we used in Figures 4 and 5 were used for Fig. 6. The values of intraretinal $[H^+]_o$ were calculated relative to average choroidal $[H^+]$ for each group.

Fig. 6 (upper row) confirmed again that diabetic retinae at 1 – 3 months were significantly more acidic than controls, but at a later time diabetics and controls were not much different on average, although diabetics demonstrated larger variability. The average H^+-profiles of longer duration diabetics (> 3 months) had their maximum at the same depth as controls (60–65 % of the retinal depth), but for diabetics of 1 – 3 months H^+-profiles peaked somewhat more distally (65–70 % of the retinal depth). However, taking into the account the size of standard deviations for the neighboring points, this difference in location of the H^+-profile peak can hardly be accepted as statistically reliable. Additionally, it appeared that the H^+-profiles of diabetics after 1 month were “sharper” than control H^+-profiles (Fig. 6, upper

Author Manuscript Author Manuscript Author Manuscript Author Manuscript

row). To confirm this visual impression the profiles were normalized, defining the maximum value as 1 and superimposing control and diabetic profiles (Fig. 6, lower row). The graphs for diabetic retinae for both time periods are found “inside” the corresponding graphs for the controls, as expected for curves with a sharper peak. To quantify the sharpness of the H^+-profiles, the profile widths when cut at half-maximum amplitude were measured. The rising front of normalized H^+-profile for diabetics 1 – 3 months reached the half-maximum amplitude at 88.4% of the retinal depth and then declined to the half-maximum at 32.7% of the retinal depth. Accordingly, the width at half-maximum amplitude of this profile was 55.7% of the retinal depth. Similarly, the width at half-maximum amplitude of normalized H^+-profile for long time diabetics (> 3 months) was 59.9% of the retinal depth. For comparison, the width at half-maximum amplitude for normalized control H^+-profiles were 64.6% (1 – 3 months) and 66.0% (> 3 months) of the retinal depth.

Another difference that is apparent from Fig. 6 is that the inner retina tended to be more acidic in the 1–3 month diabetics. The choroidal $[H^+]$ of diabetic rats was slightly more acidic (average pH = 7.38 at less than 3 months, and average pH = 7.32 at more than 3 months) than in control rats (average pH from 7.40 to 7.43 at different times). This means that the peak and inner retinal $[H^+]$ in diabetics tended to be higher not only because of the increased amplitude of profiles, but also because the baseline was a little higher. The small variations in blood pH in diabetics were not correlated with variations in their blood glucose (362 ± 63, 447 ± 70, and 394 ± 92 mg/dL at < 1 month, 1–3 months, and > 3 months, respectively).

One consistent effect of diabetes, as has been mentioned previously, was a wide range of variability of H^+-profiles, even within the same animal. Importantly, however, this variability was not random, but was spatially organized, as demonstrated by the 3-D reconstructions of the H^+ distribution in control and diabetic retinae (Fig. 7). The data for these 3-D reconstructions were obtained in a series of experiments when several (5 to 8) adjacent H^+-profiles were successfully recorded at fixed spatial intervals. Between recordings of profiles the electrode was rotated 2 degrees around the point where it penetrated the sclera. The lateral shift associated with this rotation was calculated to be 150 to 180 μm along the retinal surface, depending on the electrode orientation relatively to the vertical and horizontal axes of the rat eye. The penetrations are not absolutely parallel, so at the choroid the lateral shift was slightly larger than at the vitreal surface of the retina, but we ignore that small difference. To emphasize the differences in shape of the profiles, the 3-D graphs are not spatially isometric. A difference of 20 degrees of eccentricity in the graphs is associated with a lateral shift of 1500 – 1800 μm along the eccentricity axis, but the retinal thickness (that was recalculated into retinal depth) was 350 – 420 μm, depending on the penetration angle. Thus, in Fig. 7 the distance in the lateral (i.e. eccentricity) direction is compressed about 4 times compared to the distance in the radial (i.e. depth) direction, which serves to emphasize how the profiles change with eccentricity.

In case of control retinae (Fig. 7A–C) 3-D reconstructions of $[H^+]_o$ showed the increase of $[H^+]_o$ at the level of the outer nuclear layer (60 – 65 % of the retinal depth), with no significant lateral variations. In contrast, the most striking feature of the 3-D reconstructions in diabetic retinae (Fig. 7D–F) was considerable variation of $[H^+]_o$ in the lateral direction.

Author Manuscript Author Manuscript Author Manuscript Author Manuscript

The $[H^+]_o$ was still the highest in the outer nuclear layer,, but the maximum in the radial direction could be twice as large as the radial maximum 800 – 900 μm away (Fig 7E). It was hard to see any consistent pattern in the lateral variations of $[H^+]_o$ in diabetic retinae. In some cases the high H^+ spread from the distal retina into the proximal retina (Fig. 7D), and lateral gradients of $[H^+]_o$ were then apparent through most of the retinal depth. In other cases there was a large lateral difference in $[H^+]_o$ only in distal retina, while $[H^+]_o$ in proximal layers was about the same at all tested eccentricities (Fig. 7E). Yet, some other diabetic retinas showed local increases of $[H^+]_o$ in the proximal retina, but not in distal retina (Fig. 7F). In any case, it is obvious that the diabetes-induced elevation of $[H^+]_o$ has strongly expressed local character, so that extracellular H^+ was not only affected during diabetes, but affected differently at different retinal locations.

4. Discussion

Apart from example profiles presented in our recent paper (Dmitriev et al., 2016) this work is the first to characterize intraretinal $[H^+]_o$ in the rat retina in either control or diabetic animals. As might be expected from the similar rod-dominated character of the retinae, the profiles were similar in shape to those recorded in cats (Padnick-Silver and Linsenmeier, 2002; Yamamoto et al., 1992). The most acidic part of the retina was the outer nuclear layer, where the pH was often 7.1. The vitreal surface of the retina was always slightly more acidic than the choroid. The H^+ profiles were almost always quite smooth, even before the averaging into the 5% retinal depth bins that was performed here, and rarely showed any peaks or troughs that could be associated with the presence of blood vessels. In this respect, H^+ profiles of rats and cats are distinct from PO_2 profiles, where steep peaks and valleys are almost always found in the inner retina. The smoothness of the H^+ profiles in the inner retina suggests that the local intravascular H^+ must be close to the adjacent interstitial H^+ that we measure, and also that the levels of H^+ in the inner retina result largely from diffusion from the main source of H^+ in photoreceptors, rather than from H^+ produced in the inner retina. H^+ comes principally from anaerobic glycolysis, and this apparent lack of anaerobic glycolysis in the inner retina is consistent with the only direct attempt to measure lactate production in the inner vs. outer retina. Wang et al. (Wang et al., 1997a, b) sampled lactate from a systemic artery as well as from the vortex vein to characterize the outer retina (Wang et al., 1997a), and a vessel in the venous plexus draining the retina to characterize the inner retina (Wang et al., 1997b). They then multiplied these arteriovenous differences by the blood flow rates in the choroid and the retinal circulation respectively. The rate of lactate production was about 0.37 μmoles/min in the outer retina, and less than 0.02 μmoles/min in the inner retina

The main point of the present work, however, was to evaluate the hypothesis that the chronic hyperglycemia in diabetes would lead to a general acidification of the retina. This hypothesis was partially supported with the finding that at 1 to 3 months, the retina of diabetic rats was more acidic than the retina of age-matched controls. On average, the increased acidity was not maintained beyond this time, but the diabetics did differ from controls at all times greater than 1 month in the variability of the shape and amplitude of profiles, with much greater variability in the diabetics. This variability was spatially organized, with pockets of

Author Manuscript Author Manuscript Author Manuscript Author Manuscript

high acidity in both the inner and outer retina accounting for most of this variation within an animal.

Increased acidity of the outer retina can be explained on the basis of increased reliance on glycolytic energy production in diabetics. Photoreceptors have a well-known capacity to alter their lactate production. For example, when anaerobic glycolysis decreases, as in the light adapted retina (Winkler et al., 2008), the retina becomes less acidic (Dmitriev et al., 2016; Padnick-Silver and Linsenmeier, 2002; Yamamoto et al., 1992), and when anaerobic glycolysis increases, as in hypoxia (Ames et al., 1992; Fliesler et al., 1997; Winkler, 1995), particularly the outer retina becomes more acidic (Padnick-Silver and Linsenmeier, 2005; Yamamoto and Steinberg, 1992). Thus, it is not surprising that with access to more glucose, the photoreceptors switch to more glycolytic energy production (Winkler, 1981; Winkler et al., 1997) and the retina becomes more acidic.

Because acidosis can increase VEGF in tumors and the retina (Fukumoto et al., 2012; Shi et al., 2001; Xu et al., 2002; Zhu et al., 2009), one of the interesting questions is whether the acidosis we have observed is partially responsible for VEGF upregulation in diabetes. Proving a connection is difficult, but we and others have found increased VEGF in rats mainly at around 1 month, that is, at just the point of maximum H^+, with a decrease after this (Kirwin et al., 2009; Lau et al., 2013; Schrufer et al., 2010), again as we observe in H^+. This early increase in VEGF could be attributable to inflammation (Kern, 2007; Kirwin et al., 2009; Poulaki et al., 2004), but it is possible that acidosis also plays a role. AP-1, the transcription factor implicated in acidosis-mediated changes in VEGF (Xu et al., 2002), increases in early diabetes (Poulaki et al., 2004). Arguing against a role for acidosis in VEGF changes is the observation that the acidosis we observed was mainly in the ONL, which is not a major source of VEGF, while inner retinal acidosis did occur, but was modest. Thus, acidosis may influence VEGF in the intact retina, but may not be a major factor. Hypoxia is often associated with increased VEGF, but we were unable to detect any hypoxia in rat retina at this time (Lau and Linsenmeier, 2014), suggesting that it is unlikely to be involved in this early VEGF upregulation.

The two other main findings of the present study: 1) the lack of maintained acidosis as diabetes progresses, and 2) the increased variability in pH gradients in diabetics, need more explanation. While we do not have a complete understanding, we can generate new hypotheses.

We see two main possibilities for why acidosis is not maintained in rat as diabetes progresses. First, we know that there are progressive changes in retinal neural function in rats seen in the ERG (Li et al., 2002; Ly et al., 2011; Pautler and Ennis, 1980; Shinoda et al., 2007) and ganglion cell survival (Barber et al., 1998; Hammes et al., 1995; Kern and Barber, 2008; Qin et al., 2006). In addition, Kern and Berkowitz (Kern and Berkowitz, 2015) have recently reviewed the anatomical, biochemical and electrophysiological evidence that photoreceptors are also affected in diabetes, with increased oxidative stress as a possible underlying mechanism (Du et al., 2013). One of the most striking results concerning photoreceptors was the claim that the thickness of the outer nuclear layer in Sprague-Dawley rats was reduced by about 23% after one month of diabetes, and by half after six months

Author Manuscript Author Manuscript Author Manuscript Author Manuscript

(Park et al., 2003). Unfortunately, there were no age-matched controls in that study, so it is difficult to know whether the results were all due to diabetes or to other effects, including potentially light damage. Even without that study, however, there is substantial evidence for photoreceptor involvement in diabetes. Thus it is possible that the acidosis is not maintained in longer term diabetes due to a decrease in the ability of photoreceptors to do as much anaerobic glycolysis. This could also be the reason we found abnormal H^+ gradients in long term diabetic cats (Budzynski et al., 2005). Another possibility for the less severe acidosis at longer times is that the retina adapts and handles acid better. In animals with systemic acidosis sustained for two weeks by addition of NH_4Cl to the drinking water there is an upregulation of retinal carbonic anhydrase, acid-sensing ion channels, and the sodium-hydrogen and anion exchangers at the message level, and to the extent that it could be tested, at the protein level (Linsenmeier et al., 2015). If these changes occur in diabetes, they may lead to improvements in regulating retinal pH, and reduce the acidosis caused by diabetes. Of course both of these explanations may be partially correct.

To explain the greater variability in H^+ in diabetics within a retina, we have no specific hypothesis, but can point to the patchy and apparently random nature of vascular effects in animals and humans, such as microaneurysms, leakage and capillary dropout, as well as different manifestations in different individuals (e.g. (Engerman and Kern, 1995; Girach et al., 2006; Stitt et al., 2015)). We are not aware of a postulated mechanism for the non-uniform effect within an individual human or animal, but whatever the underlying process, the variation in pH is likely to be just another manifestation of this, reflecting differences in local H^+ production or differences in vascular clearance, or both.

As for other aspects of diabetic retinopathy, one can question the relevance of the present results to the human retina. The glucose levels, metabolic rate, and end stage in diabetic rats are quite different from those in humans, but many molecular, histological and electrophysiological changes are similar (Engerman and Kern, 1995; Lai and Lo, 2013; Obrosova et al., 2006; Samuels et al., 2015). Complicating the possibility that the retina itself is acidic in diabetes is the finding that the vitreous contains more carbonic anhydrase-1, probably from leaky blood vessels, and that this alkalinizes the vitreous and leads to further damage through a kallikrein pathway (Gao et al., 2007) Our work argues at least for paying further attention to pH in diabetes, and seeking a non-invasive way to measure retinal pH or lactate in diabetics over time, as has previously been done with MRI methods for measuring lactate in rabbit (Berkowitz et al., 1994).

5. Conclusions

Retinal acidosis begins to develop at an early stage of diabetes (1 to 3 month) in rats. However, it does not progress, and the acidity of diabetic rat retina was diminished at later stages (3 to 6 months). The diabetes-induced acidosis has strongly expressed local character. As result, the diabetic retinas show much wider variability in their $[H^+]$ distribution than controls.

Acknowledgments

Financial support

Author Manuscript Author Manuscript Author Manuscript Author Manuscript

This work was supported by NIH grant R01EY021165

Abbreviations

STZ	streptozotocin
ERG	electroretinogram
$[H^+]_o$	extracellular hydrogen concentration

References

Ames A, Li YY, Heher EG, Kimble CR. Energy metabolism of rabbit retina as related to function: high cost of Na transport. J Neuroscience. 1992; 12:840–853. [PubMed: 1312136]

Barber AJ, Lieth E, Khin SA, Antonetti DA, Buchanan AG, Gardner TW. Penn State Retina Res, G. Neural apoptosis in the retina during experimental and human diabetes - Early onset and effect of insulin. J. Clin. Invest. 1998; 102:783–791. [PubMed: 9710447]

Berkowitz BA, Bansal N, Wilson CA. Non-invasive measurement of steady-state vitreous lactate concentration. NMR in biomedicine. 1994; 7:263–268. [PubMed: 7841022]

Budzynski E, Wangsa-Wirawan N, Padnick-Silver L, Hatchell D, Linsenmeier R. Intraretinal pH in diabetic cats. Current eye research. 2005; 30:229–240. [PubMed: 15804749]

Dmitriev A, Pignatelli A, Piccolino M. Resistance of retinal extracellular space to Ca2+ level decrease: implications for the synaptic effects of divalent cations. Journal of neurophysiology. 1999; 82:283–289. [PubMed: 10400957]

Dmitriev AV, Henderson D, Linsenmeier RA. Light-induced pH changes in the intact retinae of normal and early diabetic rats. Experimental eye research. 2016; 145:148–157. [PubMed: 26639389]

Du Y, Veenstra A, Palczewski K, Kern TS. Photoreceptor cells are major contributors to diabetes-induced oxidative stress and local inflammation in the retina. Proceedings of the National Academy of Sciences of the United States of America. 2013; 110:16586–16591. [PubMed: 24067647]

Engerman RL, Kern TS. Retinopathy in animal models of diabetes. Diabetes Metab Rev. 1995; 11:109–120. [PubMed: 7555563]

Fliesler SJ, Richards MJ, Miller CY, McKay S, Winkler BS. In vitro metabolic competence of the frog retina: effects of glucose and oxygen deprivation. Exp Eye Res. 1997; 64:683–692. [PubMed: 9245897]

Fukumoto M, Nakaizumi A, Zhang T, Lentz SI, Shibata M, Puro DG. Vulnerability of the retinal microvasculature to oxidative stress: ion channel-dependent mechanisms. American Journal of Physiology-Cell Physiology. 2012; 302:C1413–C1420. [PubMed: 22345512]

Fukumura D, Xu L, Chen Y, Gohongi T, Seed B, Jain RK. Hypoxia and acidosis independently up-regulate vascular endothelial growth factor transcription in brain tumors in vivo. Cancer research. 2001; 61:6020–6024. [PubMed: 11507045]

Gao BB, Clermont A, Rook S, Fonda SJ, Srinivasan VJ, Wojtkowski M, Fujimoto JG, Avery RL, Arrigg PG, Bursell SE, Aiello LP, Feener EP. Extracellular carbonic anhydrase mediates hemorrhagic retinal and cerebral vascular permeability through prekallikrein activation. Nature medicine. 2007; 13:181–188.

Girach A, Manner D, Porta M. Diabetic microvascular complications: can patients at risk be identified? A review. Int J Clin Pract. 2006; 60:1471–1483. [PubMed: 17073842]

Hammes HP, Federoff HJ, Brownlee M. Nerve growth factor prevents both neuroretinal programmed cell death and capillary pathology in experimental diabetes. Mol Med. 1995; 1:527–534. [PubMed: 8529118]

Holmes JM, Zhang S, Leske DA, Lanier WL. Carbon dioxide-induced retinopathy in the neonatal rat. Current eye research. 1998; 17:608–616. [PubMed: 9663850]

Holmes JM, Zhang S, Leske DA, Lanier WL. Metabolic acidosis-induced retinopathy in the neonatal rat. Invest Ophthalmol Vis Sci. 1999; 40:804–809. [PubMed: 10067989]

Author Manuscript Author Manuscript Author Manuscript Author Manuscript

Kern TS. Contributions of inflammatory processes to the development of the early stages of diabetic retinopathy. Experimental diabetes research. 2007; 2007:95103. [PubMed: 18274606]

Kern TS, Barber AJ. Retinal ganglion cells in diabetes. The Journal of physiology. 2008; 586:4401–4408. [PubMed: 18565995]

Kern TS, Berkowitz BA. Photoreceptors in diabetic retinopathy. J Diabetes Investig. 2015; 6:371–380.

Kirwin SJ, Kanaly ST, Linke NA, Edelman JL. Strain-dependent increases in retinal inflammatory proteins and photoreceptor FGF-2 expression in streptozotocin-induced diabetic rats. Invest Ophthalmol Vis Sci. 2009; 50:5396–5404. [PubMed: 19474406]

Lai AK, Lo AC. Animal models of diabetic retinopathy: summary and comparison. J Diabetes Res. 2013; 2013:106594. [PubMed: 24286086]

Lau JC, Kroes RA, Moskal JR, Linsenmeier RA. Diabetes changes expression of genes related to glutamate neurotransmission and transport in the Long-Evans rat retina. Molecular vision. 2013; 19:1538–1553. [PubMed: 23878504]

Lau JC, Linsenmeier RA. Oxygen consumption and distribution in the Long-Evans rat retina. Experimental eye research. 2012; 102:50–58. [PubMed: 22828049]

Lau JC, Linsenmeier RA. Increased intraretinal PO2 in short-term diabetic rats. Diabetes. 2014; 63:4338–4342. [PubMed: 25028524]

Leske DA, Wu J, Fautsch MP, Karger RA, Berdahl JP, Lanier WL, Holmes JM. The role of VEGF and IGF-1 in a hypercarbic oxygen-induced retinopathy rat model of ROP. Mol Vis. 2004; 10:43–50. [PubMed: 14758338]

Li Q, Zemel E, Miller B, Perlman I. Early retinal damage in experimental diabetes: electroretinographical and morphological observations. Experimental eye research. 2002; 74:615–625. [PubMed: 12076083]

Linsenmeier RA, Dreffs A, Henderson D, Antonetti DA. Increased Retinal Expression of Carbonic Anhydrase, Anion and Proton Exchanger in Response to Systemic Acidosis. Investigative Ophthalmology & Visual Science. 2015; 56

Ly A, Yee P, Vessey KA, Phipps JA, Jobling AI, Fletcher EL. Early inner retinal astrocyte dysfunction during diabetes and development of hypoxia, retinal stress, and neuronal functional loss. Investigative ophthalmology & visual science. 2011; 52:9316–9326. [PubMed: 22110070]

Obrosova IG, Drel VR, Kumagai AK, Szabo C, Pacher P, Stevens MJ. Early diabetes-induced biochemical changes in the retina: comparison of rat and mouse models. Diabetologia. 2006; 49:2525–2533. [PubMed: 16896942]

Padnick-Silver L, Linsenmeier RA. Quantification of in vivo anaerobic metabolism in the normal cat retina through intraretinal pH measurements. Visual neuroscience. 2002; 19:793–806. [PubMed: 12688673]

Padnick-Silver L, Linsenmeier RA. Effect of hypoxemia and hyperglycemia on pH in the intact cat retina. Arch Ophthalmol. 2005; 123:1684–1690. [PubMed: 16344440]

Park SH, Park JW, Park SJ, Kim KY, Chung JW, Chun MH, Oh SJ. Apoptotic death of photoreceptors in the streptozotocin-induced diabetic rat retina. Diabetologia. 2003; 46:1260–1268. [PubMed: 12898017]

Pautler EL, Ennis SR. The effect of induced diabetes on the electroretinogram components of the pigmented rat. Investigative ophthalmology & visual science. 1980; 19:702–705. [PubMed: 7380629]

Poulaki V, Joussen AM, Mitsiades N, Mitsiades CS, Iliaki EF, Adamis AP. Insulin-like growth factor-I plays a pathogenetic role in diabetic retinopathy. The American journal of pathology. 2004; 165:457–469. [PubMed: 15277220]

Qin Y, Xu G, Wang W. Dendritic abnormalities in retinal ganglion cells of three-month diabetic rats. Current eye research. 2006; 31:967–974. [PubMed: 17114122]

Samuels IS, Bell BA, Pereira A, Saxon J, Peachey NS. Early retinal pigment epithelium dysfunction is concomitant with hyperglycemia in mouse models of type 1 and type 2 diabetes. Journal of neurophysiology. 2015; 113:1085–1099. [PubMed: 25429122]

Scarinci F, Jampol LM, Linsenmeier RA, Fawzi AA. Association of Diabetic Macular Nonperfusion With Outer Retinal Disruption on Optical Coherence Tomography. JAMA Ophthalmol. 2015; 133:1036–1044. [PubMed: 26158562]

Author Manuscript Author Manuscript Author Manuscript Author Manuscript

Schrufer TL, Antonetti DA, Sonenberg N, Kimball SR, Gardner TW, Jefferson LS. Ablation of 4E-BP1/2 prevents hyperglycemia-mediated induction of VEGF expression in the rodent retina and in Muller cells in culture. Diabetes. 2010; 59:2107–2116. [PubMed: 20547975]

Shi Q, Le X, Wang B, Abbruzzese JL, Xiong Q, He Y, Xie K. Regulation of vascular endothelial growth factor expression by acidosis in human cancer cells. Oncogene. 2001; 20:3751–3756. [PubMed: 11439338]

Shinoda K, Rejdak R, Schuettauf F, Blatsios G, Volker M, Tanimoto N, Olcay T, Gekeler F, Lehaci C, Naskar R, Zagorski Z, Zrenner E. Early electroretinographic features of streptozotocin-induced diabetic retinopathy. Clinical & experimental ophthalmology. 2007; 35:847–854. [PubMed: 18173414]

Stitt AW, Curtis TM, Chen M, Medina RJ, McKay GJ, Jenkins A, Gardiner TA, Lyons TJ, Hammes HP, Simo R, Lois N. The progress in understanding and treatment of diabetic retinopathy. Progress in retinal and eye research. 2015

Wang L, Tornquist P, Bill A. Glucose metabolism in pig outer retina in light and darkness. Acta physiologica Scandinavica. 1997a; 160:75–81. [PubMed: 9179314]

Wang L, Tornquist P, Bill A. Glucose metabolism of the inner retina in pigs in darkness and light. Acta physiologica Scandinavica. 1997b; 160:71–74. [PubMed: 9179313]

Winkler BS. Glycolytic and oxidative metabolism in relation to retinal function. J Gen Physiol. 1981; 77:667–692. [PubMed: 6267165]

Winkler, BS. A quantitative assessment of glucose metabolism in the isolated rat retina. In: Christen, Y.; Doly, M.; Droy-Lefaix, M., et al., editors. Les Seminaires ophthalmologiques d'IPSEN, Vision et adaptation. Paris: Elsevier; 1995. p. 78-96.

Winkler BS, Arnold MJ, Brassell MA, Sliter DR. Glucose dependence of glycolysis, hexose monophosphate shunt activity, energy status, and the polyol pathway in retinas isolated from normal (nondiabetic) rats. Invest Ophthalmol Vis Sci. 1997; 38:62–71. [PubMed: 9008631]

Winkler BS, Starnes CA, Twardy BS, Brault D, Taylor RC. Nuclear magnetic resonance and biochemical measurements of glucose utilization in the cone-dominant ground squirrel retina. Invest Ophthalmol Vis Sci. 2008; 49:4613–4619. [PubMed: 18566456]

Xu L, Fukumura D, Jain RK. Acidic extracellular pH induces vascular endothelial growth factor (VEGF) in human glioblastoma cells via ERK1/2 MAPK signaling pathway: mechanism of low pH-induced VEGF. J Biol Chem. 2002; 277:11368–11374. [PubMed: 11741977]

Yamamoto F, Borgula GA, Steinberg RH. Effects of light and darkness on pH outside rod photoreceptors in the cat retina. Exp Eye Res. 1992; 54:685–697. [PubMed: 1623953]

Yamamoto F, Steinberg RH. Effects of systemic hypoxia on pH outside rod photoreceptors in the cat retina. Exp Eye Res. 1992; 54:699–709. [PubMed: 1623954]

Zhu D, Xu X, Zheng Z, Gu Q. Regulation of vascular endothelial growth factor and pigment epithelium-derived factor in rat retinal explants under retinal acidification. Eye (London, England). 2009; 23:2105–2111.

Author Manuscript Author Manuscript Author Manuscript Author Manuscript

Highlights

- We hypothesized that diabetic retinae would be acidic due to increased glycolysis.
- We measured $[H^+]_o$ in retinae of control and diabetic rats with H^+ microelectrodes.
- In controls, $[H^+]_o$ in the outer nuclear layer is about 30 nM higher than in blood.
- Retinae were more acidic from 1 to 3 months of diabetes, but not before or after.
- $[H^+]_o$ was more variable in diabetic retinae, both within and between animals.

Author Manuscript Author Manuscript Author Manuscript Author Manuscript

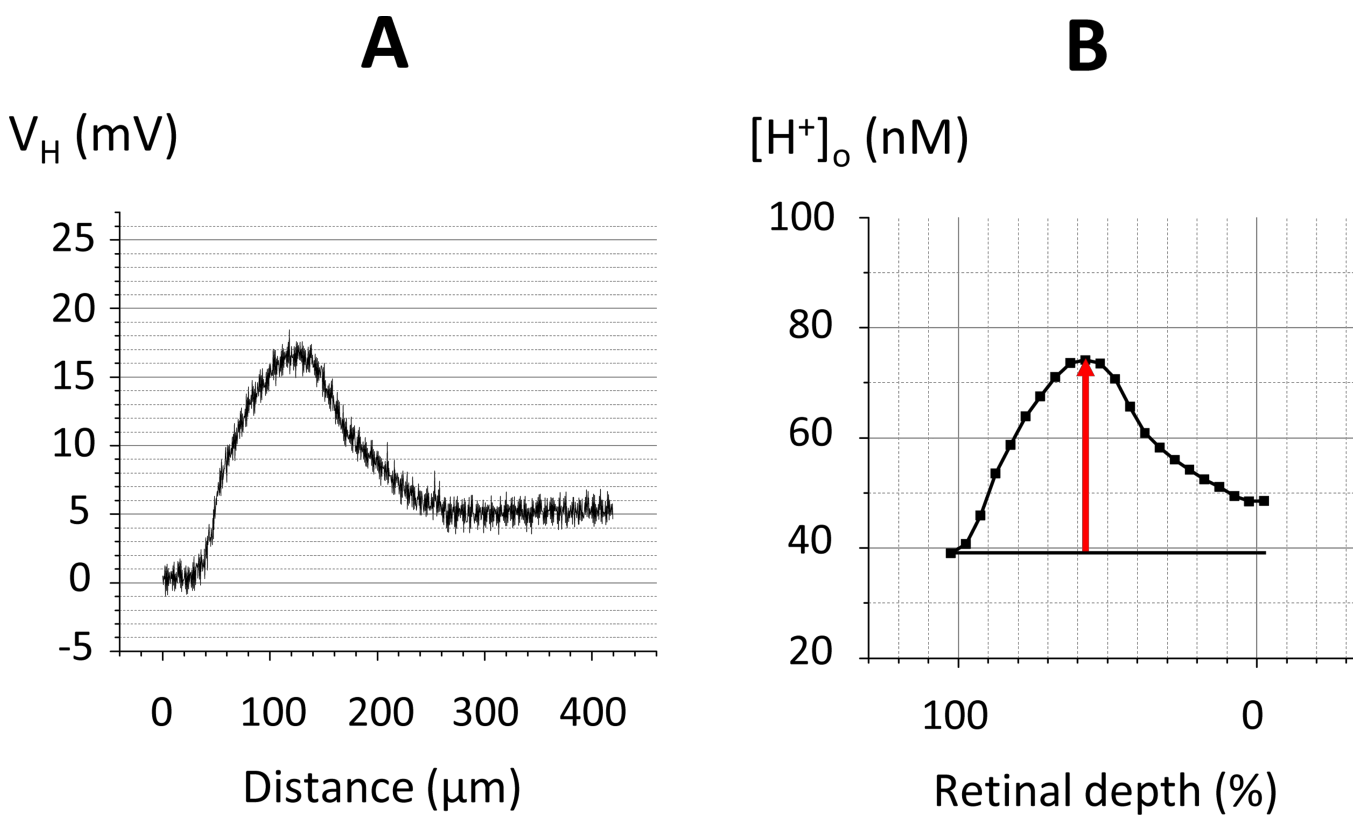

Figure 1. Converting the voltage of the H^+-selective microelectrode (A) into a H^+-profile (B)

A: The H^+ voltage of the H^+-selective microelectrode (which is the difference between the voltages of the ion-selective and reference barrels of the double barreled micropipette) consists of 840 data points obtained during 7 min of recording (2 Hz) when the electrode was continuously withdraw from the choroid to the vitreous. **B:** The final H^+-profile that represents the calculated extracellular H^+ concentration plotted against the normalized retinal depth consists of 22 data points, 20 for average $[H^+]_o$ in thin retinal sections (each accounting for 5% of total retinal depth), plus the average $[H^+]$ in the choroid and the vitreous just outside of the retina. The horizontal line marks the choroidal $[H^+]$; the arrow shows the amplitude of the H^+-profile.

Author Manuscript Author Manuscript Author Manuscript Author Manuscript

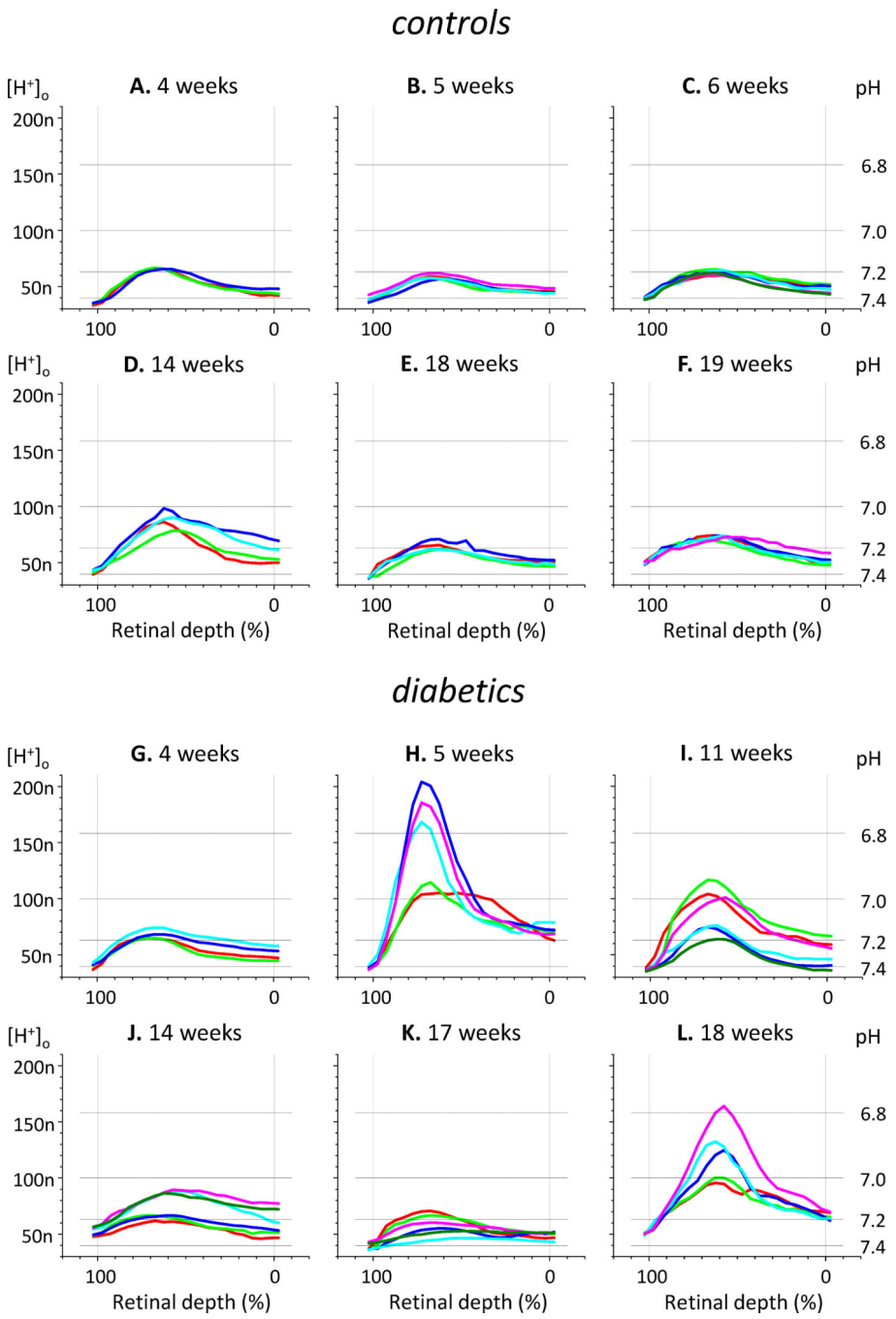

Figure 2. Samples of H^+-profiles measured in control (A–F) and diabetic (G–L) rats

Each part of the figure represents data obtained on an individual rat, and shows 3 to 6 H^+-profiles per animal. The time after STZ injection (or vehicle injection in case of controls) is marked above each graph. Here and in all other figures $[H^+]_o$ is presented in nM; for reference in this figure grid lines mark corresponding pH values. The scale of the Y-axis is the same for all parts of the figure; to prevent overcrowding of the figure the labels for $[H^+]_o$ are shown only for parts A, D, G, and J, and the labels for pH are shown only for parts C, F, I, and L.

Author Manuscript Author Manuscript Author Manuscript Author Manuscript

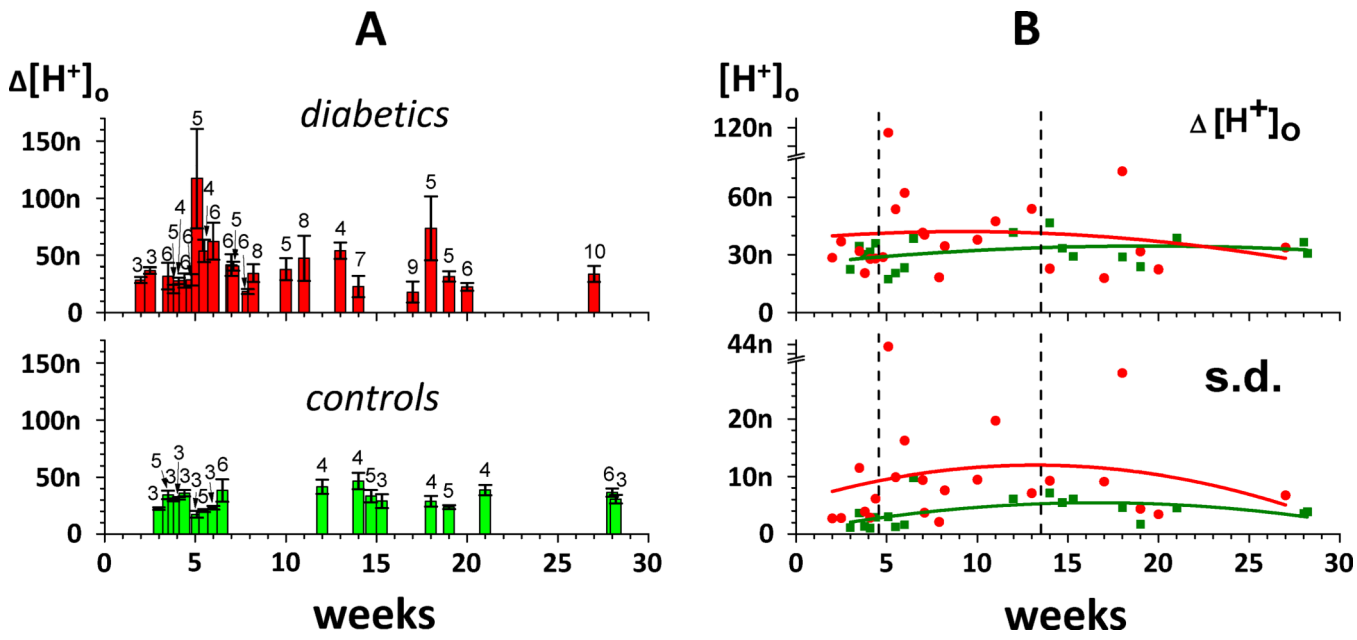

Figure 3. Comparison of H^+-profile amplitudes in control (green) and diabetic (red) retinae

A: The mean values of H^+-profile amplitudes (± s.d.) from individual rats plotted against time (in weeks) after initiation of diabetes (or injection of a vehicle for control). Green bars – controls, red bars – diabetics. Numbers of profiles averaged in each rat are marked above corresponding bars. When 2 or more data points were obtained at the same time (the same week), the corresponding bars were shifted left or right for a fraction of the week for better visual presentation.

B: Comparison of the mean values (upper part) and standard deviations (lower part) of H^+-profiles from control (green) and diabetic (red) animals. The curves (green for controls, red for diabetics) are polynomial fits of 2nd order. Vertical dashed lines marked the borders of 3 periods: 2 – 4 weeks (less than 1 month), 5 – 13 weeks (1 – 3 months), and 14 – 30 weeks (more than 3 months). Note breaks in both Y axes (from 80 to 105 nM in the upper part of the figure and from 30 to 41 nM in the lower part of the figure) which help accommodate data points at the 5th week.

Author Manuscript Author Manuscript Author Manuscript Author Manuscript

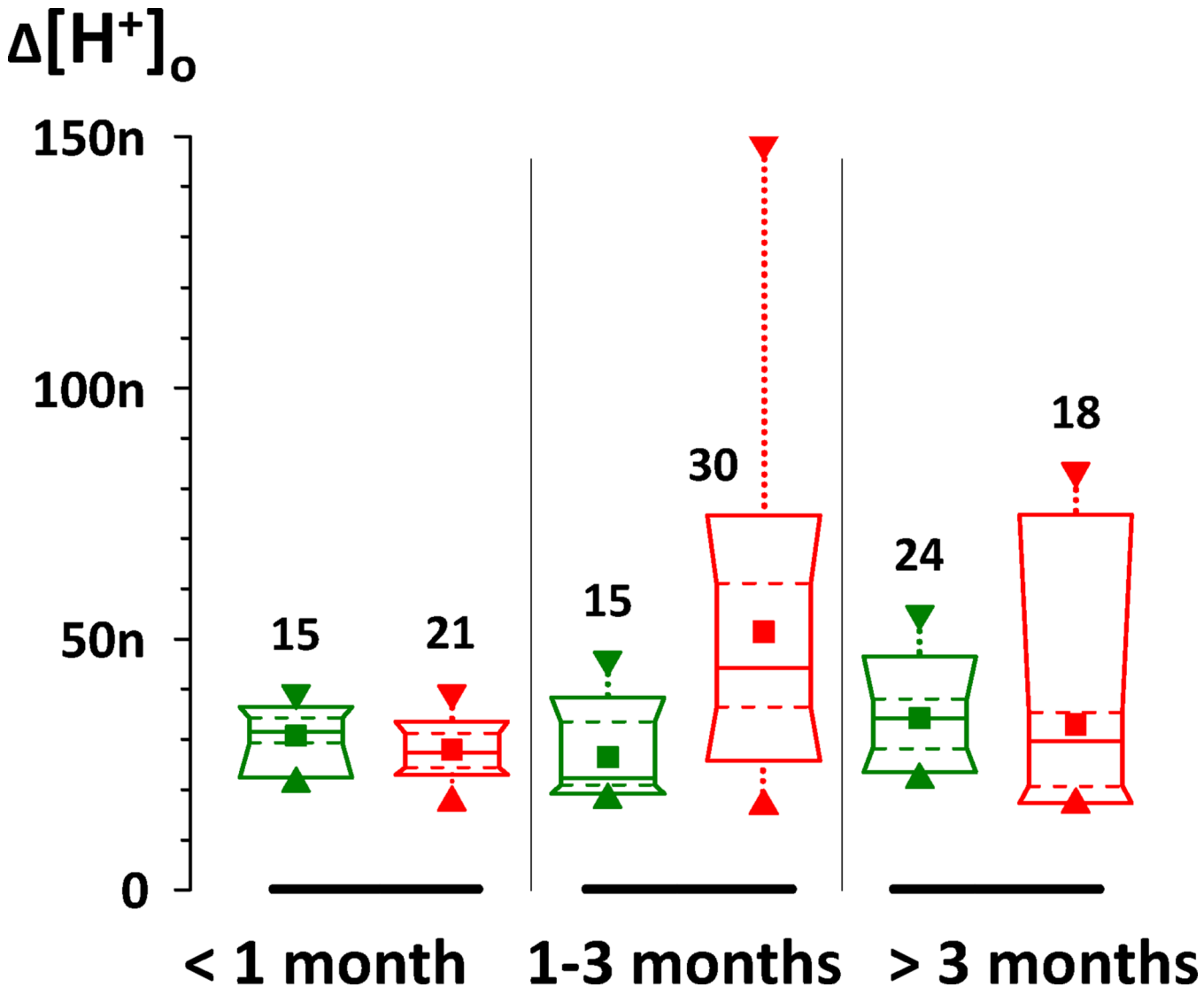

Figure 4. Box charts of H^+-profile amplitudes from control (green) and diabetic (red) animals

Data presented separately for 3 time periods: shorter than 1 month (on the left), 1 to 3 months (in the middle), and 3 to 6 months (on the right). ■ - the mean of profiles recorded from different rats (3 profiles per rat); ▲ – minimum;▼ – maximum; boxes cover from 10% to 90% of the values in each group; solid lines in boxes – median; dashed lines in boxes are 25% and 75%. Numbers of profiles in each group are marked near corresponding boxes.

Author Manuscript Author Manuscript Author Manuscript Author Manuscript

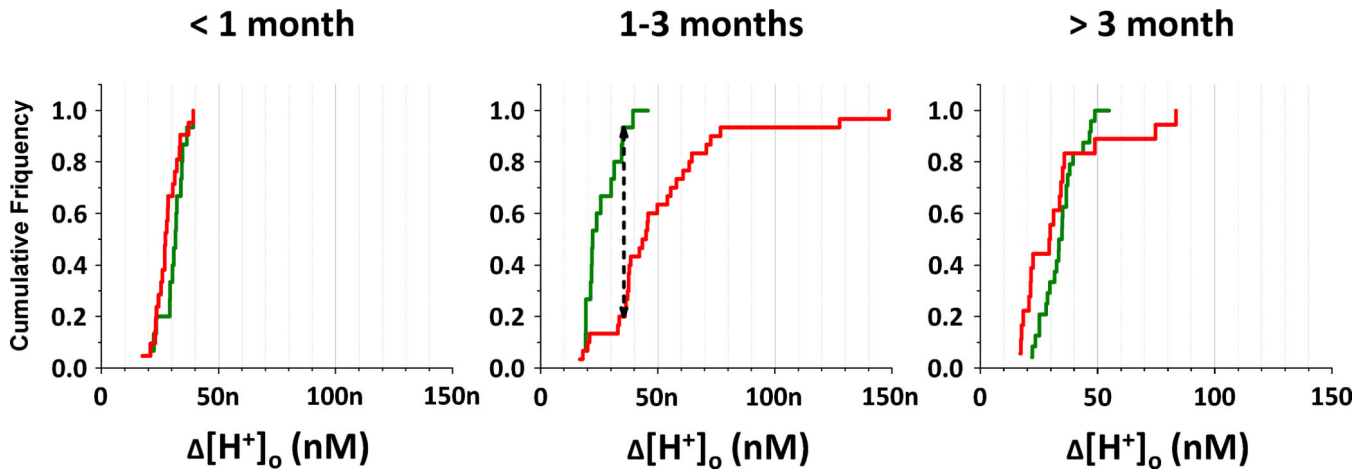

Figure 5. Cumulative distributions of H^+-profile amplitudes from control (green) and diabetic (red) rats

Data presented separately for 3 time periods: shorter than 1 month (on the left), 1 to 3 months (in the middle), and 3 to 6 months (on the right). On the graphs cumulative frequency is plotted against amplitude of the H^+-profiles. The black dashed arrow in the middle graph is the KS statistic $D_{n1,n2}$; it is equal to 0.733. In order to reject the null hypothesis (control and diabetics are not different) $D_{n1,n2}$ should be larger than $c(\alpha)*\sqrt{(n1+n2)/(n1*n2)}$, where $c(\alpha)$ is a coefficient at a certain level of significance α (equal to 1.95 at $\alpha = 0.001$), and n1 and n2 are numbers of profiles in the control and diabetic groups (15 and 30, respectively). The numerical value of $c(\alpha)*\sqrt{(n1+n2)/(n1*n2)}$ in for $\alpha=0.001$ is 0.616. For these data $D_{n1,n2} > c(\alpha)*\sqrt{(n1+n2)/(n1*n2)}$, i.e., the difference between diabetics and controls is statistically significant with $P < 0.001$.

Author Manuscript
Author Manuscript
Author Manuscript
Author Manuscript

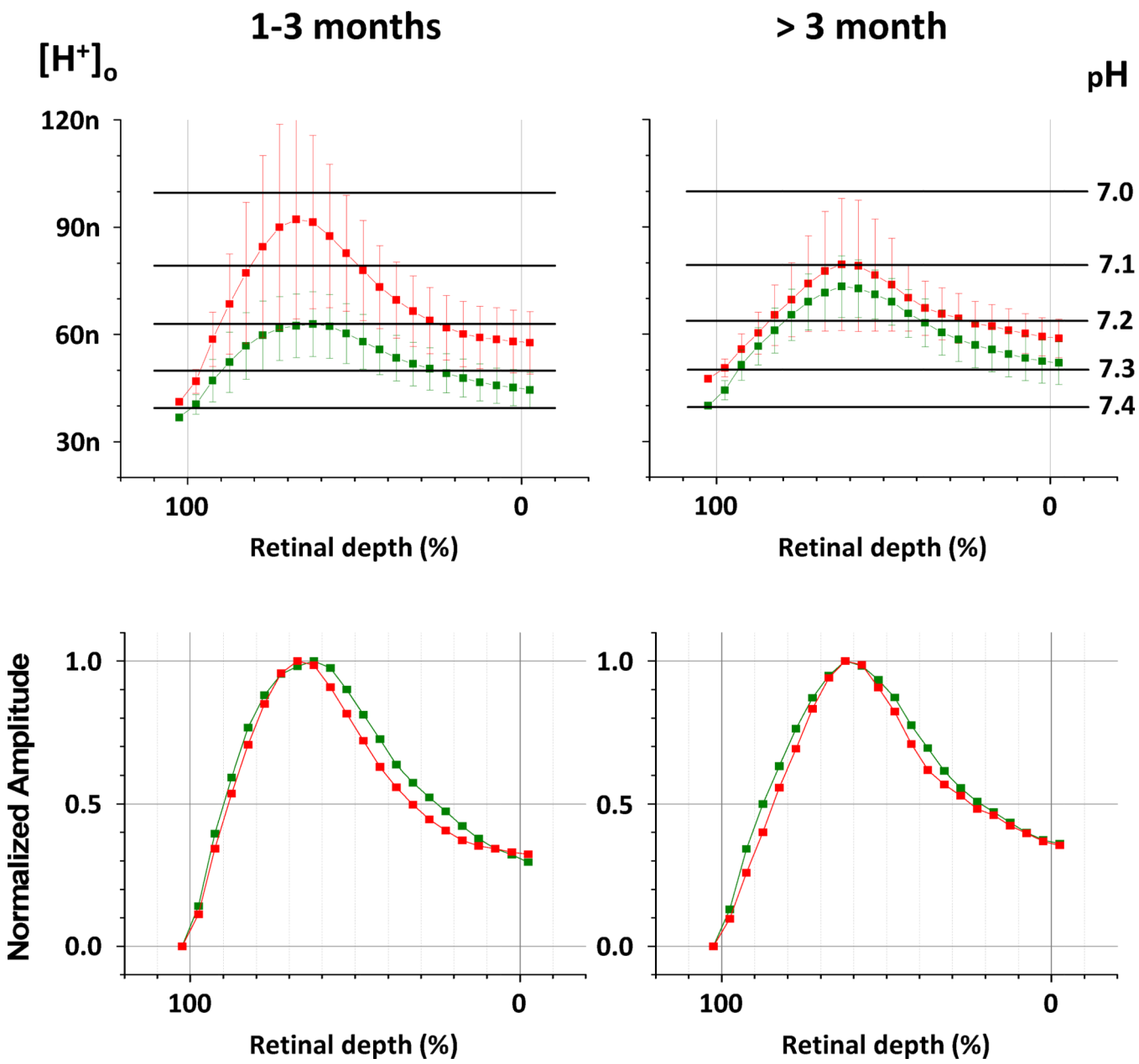

Figure 6. Average H^+-profiles in control (green) and diabetic (red) retinae

Control and diabetic H^+-profiles (mean ± s.d.) for 2 time periods: 1 to 3 months (left column), and 3 to 6 months (right column). Upper row – average H^+-profiles (mean ± s.e.m.). Numbers of individual profiles used for averaging: 1 – 3 month diabetics = 30, more than 3 month diabetics = 18, 1 – 3 month controls = 15, more than 3 month controls = 24. Lower row – normalized average H^+-profiles, when each point is presented relative to maximum amplitude.

Author Manuscript Author Manuscript Author Manuscript Author Manuscript

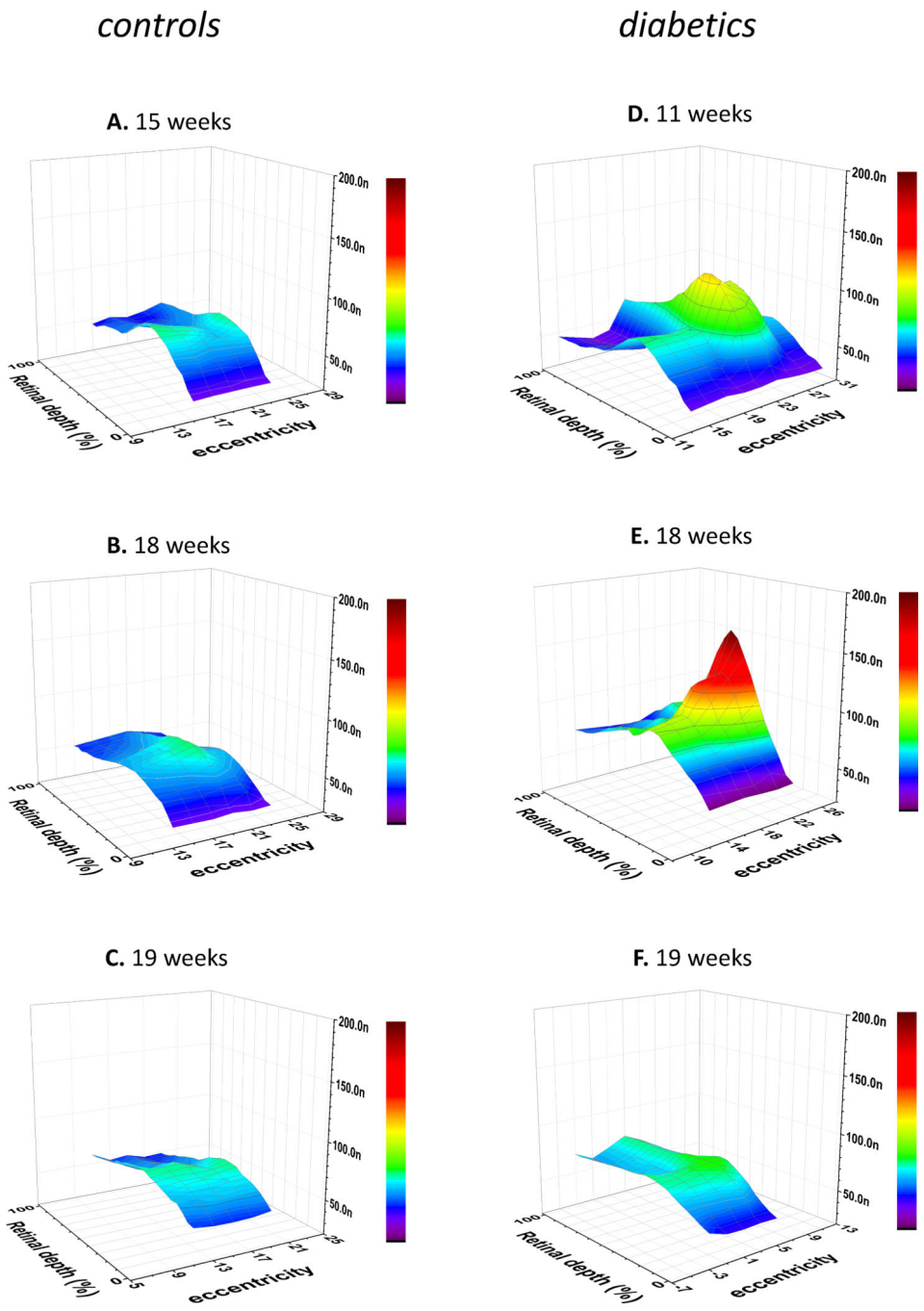

Figure 7. 3D presentation of [H^+] distribution in control (A–C) and diabetic (D–F) retinae

Each part of the figure represents data obtained on individual rats, 5 to 8 H^+-profiles per animal. The value of local $[H^+]_o$ was plotted against two space axes – retinal depth (in %) and eccentricity (in degrees of electrode rotation about the wall of the eye). The time after STZ injection (or vehicle injection in case of control) is marked above each graph. To emphasize the lateral gradients, the distance in the tangential direction is compressed about 4 times compared to the distance in the radial direction.